

Stability of trapped degenerate dipolar Bose and Fermi gases

S. K. Adhikari

Instituto de Física Teórica, UNESP - Universidade Estadual Paulista,
01.140-070 São Paulo, São Paulo, Brazil

Abstract. Trapped degenerate dipolar Bose and Fermi gases of cylindrical symmetry with the polarization vector along the symmetry axis are only stable for the strength of dipolar interaction below a critical value. In the case of bosons, the stability of such a dipolar Bose-Einstein condensate (BEC) is investigated for different strengths of contact and dipolar interactions using variational approximation and numerical solution of a mean-field model. In the disk shape, with the polarization vector perpendicular to the plane of the disk, the atoms experience an overall dipolar repulsion and this fact should contribute to the stability. However, a complete numerical solution of the dynamics leads to the collapse of a strongly disk-shaped dipolar BEC due to the long-range anisotropic dipolar interaction. In the case of fermions, the stability of a trapped single-component degenerate dipolar Fermi gas is studied including the Hartree-Fock exchange and Brueckner-Goldstone correlation energies in the local-density approximation valid for a large number of atoms. Estimates for the maximum allowed number of polar Bose and Fermi molecules in BEC and degenerate Fermi gas are given.

PACS numbers: 03.75.Hh, 03.75.Ss, 03.75.Kk, 05.30.Fk

1. Introduction

After the experimental realization of Bose-Einstein condensate (BEC) of ^{52}Cr [1, 2], ^{164}Dy [3], and ^{168}Er [4] atoms and a single-component degenerate Fermi gas of ^{161}Dy [5] atoms with large magnetic dipolar interaction, there has been new interest in the theoretical and experimental studies of degenerate gases. Polar Bose [6] and Fermi [7] molecules with much larger permanent electric dipole moment are also being considered for future experiments. The anisotropic long-range nonlocal dipolar interaction acting in all partial waves in these atoms and molecules is distinct from isotropic S -wave contact interaction. Due to the anisotropic nonlocal nature of dipolar interaction, the stability of a dipolar BEC depends on the number of atoms, dipolar interaction and scattering length as well as, reasonably strongly and distinctly, on the trap geometry [2, 8, 10]. For example, in the nondipolar case the spherically symmetric configuration is the most stable one [11] and accommodate the largest number of atoms, whereas in the dipolar case the disk-shaped configuration is the most stable one.

One advantage in investigating the effect of dipolar interaction in a single-component degenerate dipolar Fermi gas over that in a dipolar BEC is the remarkable stability of the former. Due to three-body loss via molecule formation, a BEC can be easily destroyed. The three-body loss is highly suppressed in a degenerate Fermi gas due to Pauli repulsion among identical fermions and this system is unconditionally stable in the absence of dipolar interaction. Nevertheless, in the presence of dipolar interaction beyond a certain strength, both the trapped BEC [8, 9, 10] and the degenerate Fermi gas [12, 13] are unstable because of possible collapse. New mechanism and route to collapse open up in the presence of dipolar interaction because of atomic interaction in non- S (angular momentum $L \neq 0$) waves. Dipolar BECs are immediately distinguishable from those with purely contact interaction by their strong and distinct shape and stability dependence on the trapping geometry. In the case of a trapped dipolar BEC of ^{52}Cr atoms, anisotropic D wave collapse has been studied both theoretically and experimentally [14]. Structure formation during the collapse has been studied in a single-component [10], in a binary dipolar BEC [15], and in a dipolar droplet bound in a nondipolar BEC [16].

We undertake a systematic study of the stability of a trapped dipolar BEC and of a trapped degenerate dipolar Fermi gas, both with cylindrical symmetry. The polarization direction is always taken along the axial symmetry direction. Similar studies [11] of nondipolar BECs illustrated the effect of the trapping symmetry and atomic contact attraction on stability. We present stability plots of a trapped dipolar BEC for varying number of atoms, scattering length, dipolar interaction, and trap symmetry. Such stability plots should aid in the future planning of experiments. The repulsive atomic contact interaction as well as strongly disk-shaped trap should facilitate stability and it is intuitively expected that these could lead to the absolute stability of the dipolar BEC and this possibility is supported by a Lagrangian variational analysis of the system. However, a complete dynamical treatment shows that for an increased dipolar

interaction, a cylindrically trapped dipolar BEC should collapse independent of the underlying trap symmetry and of a large atomic contact repulsion. In the case of polar molecules, under the usual condition of trapping, the number of molecules in a stable BEC could be very small, typically, less than a hundred. The number of molecules in a stable BEC can be increased by considering a significantly weaker trap with much reduced trapping frequency.

We also study, using the real-time routine, the dynamical nature of local collapse in dipolar BECs induced by a change of dipolar interaction, as opposed to global collapse in nondipolar BEC induced by a change in contact interaction managed by the Feshbach resonance technique [17]. The dipolar interaction can be controlled experimentally by a rotating orienting field [18] to initiate the collapse while maintaining a constant atomic interaction. The dipolar interaction is most prominent in disk and cigar shapes and we consider only these shapes. In both cases we evidence local collapse and not a global collapse to the trap center. In cigar shape, the dipolar BEC is first elongated and compressed on the axial symmetry direction and with further compression, centers of collapse develop along this axis and eventually the collapsed state with small pieces of BEC occupies a large extension along the symmetry axis. In disk shape, due to increased dipolar repulsion, the disk-shaped BEC first takes the shape of a donut and individual centers of collapse appear on this donut. Eventually, after the collapse and breaking up, small pieces of BEC occupy the whole volume of the entire initial disk.

The stability of a trapped degenerate dipolar Fermi gas has been studied by several groups. Miyakawa *et al.* [13] showed that the Fock exchange term causes a deformation of the Fermi surface in the presence of anisotropic dipolar interaction which plays a crucial role in the stability. They introduce a variational Wigner function to describe the deformation of the Fermi gas in phase space and use it to study the stability. Zhang and Yi [12] considered the deformed Fermi surface in the form of an ellipsoid and provided a variational and numerical solution of stability. Liu and Yin [19] further included a Brueckner-Goldstone (BG) correlation correction to the energy of a degenerate dipolar Fermi gas with deformed Fermi surface and studied its stability. However, we find contradiction among some of the studies and lack of physical plausibility of some of the results. In view of this, we find the necessity of a critical investigation of this problem.

In Sec. 2.1 we present a brief description of the mean-field model of the dipolar BEC which we use in this work. We also present an analytical variational approximation of the same. The present theoretical formulation for the degenerate dipolar Fermi gas in local-density approximation (LDA) [20] is formulated in Sec. 2.2. An explicit contribution of Fock deformation to Fermi surface and of the BG correlation correction to energy and chemical potential is included in the LDA. We present a simple scaled form of the model which we use in numerical study. In Sec. 3.1, we present numerical results for the stability of a dipolar BEC and in Sec. 3.2 the same for the degenerate dipolar Fermi gas. Finally, in Sec. IV we present a summary of our study.

2. Analytical Consideration

2.1. Mean-field model for dipolar BEC

A dipolar BEC of N atoms, each of mass m satisfies the mean-field Gross-Pitaevskii (GP) equation [1]

$$i\hbar \frac{\partial}{\partial t} \phi(\mathbf{r}) = \left[-\frac{\hbar^2 \nabla^2}{2m} + \frac{m\omega^2}{2} (\lambda^{-2/3} \rho^2 + \lambda^{4/3} z^2) + \frac{4\pi\hbar^2 a N}{m} \phi^2(\mathbf{r}) + N \int U_{\text{dd}}(\mathbf{r} - \mathbf{r}') \phi^2(\mathbf{r}') d\mathbf{r}' \right] \phi(\mathbf{r}), \quad (1)$$

with $\phi(\mathbf{r})$ the wave function, a the atomic scattering length, $n(\mathbf{r}) \equiv \phi^2(\mathbf{r})$ the BEC density normalized as $\int n(\mathbf{r}) d\mathbf{r} = 1$, $\lambda = \omega_z/\omega_\rho$ is the trap aspect ratio, $\omega = (\omega_\rho^2 \omega_z)^{1/3}$ is the average trap angular frequency, where ω_ρ and ω_z are the angular frequencies of radial and axial traps. The dipolar interaction between two atoms at \mathbf{r} and \mathbf{r}' in (1) is taken as

$$U_{\text{dd}}(\mathbf{R}) = \frac{\mu_0 \mu_d^2}{4\pi} \frac{(1 - 3 \cos^2 \theta)}{R^3} \equiv \frac{\mu_0 \mu_d^2}{4\pi} V_{\text{dd}}(\mathbf{R}), \quad \mathbf{R} = \mathbf{r} - \mathbf{r}', \quad (2)$$

where θ is the angle between the vector \mathbf{R} and the polarization direction z , μ_0 is the permeability of free space and μ_d is the magnetic dipole moment of each atom. In case of polar molecules, each of electric dipole moment d , the prefactor in (2) is $d^2/(4\pi\epsilon_0)$, where ϵ_0 is the permittivity of vacuum. To compare the strengths of atomic short-range and dipolar interactions, the dipolar interaction is often expressed in terms of the length scale $a_{\text{dd}} = m\mu_0\mu_d^2/(12\pi\hbar^2)$; for polar molecules $a_{\text{dd}} = md^2/(12\pi\epsilon_0\hbar^2)$. Using this length scale, it is convenient to write the dipolar GP equation (1) in the following dimensionless form

$$i\hbar \frac{\partial}{\partial t} \phi(\mathbf{r}, t) = \left[-\frac{\nabla^2}{2} + \frac{1}{2} (\lambda^{-2/3} \rho^2 + \lambda^{4/3} z^2) + 4\pi a N \phi^2(\mathbf{r}) + 3a_{\text{dd}} N \int V_{\text{dd}}(\mathbf{r} - \mathbf{r}') \phi^2(\mathbf{r}') d\mathbf{r}' \right] \phi(\mathbf{r}, t). \quad (3)$$

In (3) energy, length, density $n(\mathbf{r})$ and time t are expressed in units of oscillator energy $\hbar\omega$, oscillator length $l_0 \equiv \sqrt{\hbar/m\omega}$, l_0^{-3} , and ω^{-1} , respectively.

A partial understanding of the existence of a stable trapped BEC can be obtained from a variational approximation to (3) with the following ansatz [21, 22]

$$n(\mathbf{r}) = \frac{1}{\pi^{3/2} w_\rho^2 w_z} \exp \left[-\frac{\rho^2}{w_\rho^2} - \frac{z^2}{w_z^2} \right], \quad (4)$$

where w_ρ and w_z are the variational widths along radial ρ and axial z directions. The effective energy per particle of a stationary state propagating as $\phi(\mathbf{r}, t) \sim \exp(-i\mu t/\hbar) \varphi(\mathbf{r})$, where μ is the chemical potential, can be written as

$$E = \int d\mathbf{r} \left[\frac{1}{2} |\nabla_{\mathbf{r}} \varphi(\mathbf{r})|^2 + \frac{1}{2} (\lambda^{-2/3} \rho^2 + \lambda^{4/3} z^2) \varphi^2(\mathbf{r}) + 2\pi a N \varphi^4(\mathbf{r}) + \frac{3a_{\text{dd}} N}{2} \int d\mathbf{r}' \varphi^2(\mathbf{r}) \varphi^2(\mathbf{r}') V_{\text{dd}}(\mathbf{r} - \mathbf{r}') \right]. \quad (5)$$

With the density (4), the effective energy (5) becomes

$$E = \frac{1}{2w_\rho^2} + \frac{1}{4w_z^2} + \frac{w_\rho^2}{2\lambda^{2/3}} + \frac{\lambda^{4/3}w_z^2}{4} + \frac{N[a - a_{\text{dd}}f(\kappa)]}{\sqrt{2\pi}w_\rho^2w_z}, \quad (6)$$

where $\kappa = w_\rho/w_z$ and

$$f(\kappa) = \frac{1 + 2\kappa^2}{1 - \kappa^2} - \frac{3\kappa^2 \tanh^{-1}\sqrt{1 - \kappa^2}}{(1 - \kappa^2)^{3/2}}. \quad (7)$$

The stable stationary states correspond to a global minimum of energy (6) for the ground state BEC. Maxima and saddle points have been identified to be excited stationary states [23]. The widths of the ground state BEC with Gaussian ansatz can be obtained by a minimization of energy (6) by $\partial E/\partial w_z = \partial E/\partial w_\rho = 0$ [2, 22]:

$$\frac{w_\rho}{\lambda^{2/3}} = \frac{1}{w_\rho^3} + \frac{[a - a_{\text{dd}}g(\kappa)]/2}{\sqrt{2\pi}} \frac{2N}{w_\rho^3w_z}, \quad (8)$$

$$w_z\lambda^{4/3} = \frac{1}{w_z^3} + \frac{[a - a_{\text{dd}}h(\kappa)]}{\sqrt{2\pi}} \frac{2N}{w_\rho^2w_z^2}, \quad (9)$$

where

$$g(\kappa) = \frac{2 - 7\kappa^2 - 4\kappa^4}{(1 - \kappa^2)^2} + \frac{9\kappa^4 \tanh^{-1}\sqrt{1 - \kappa^2}}{(1 - \kappa^2)^{5/2}}, \quad (10)$$

$$h(\kappa) = \frac{1 + 10\kappa^2 - 2\kappa^4}{(1 - \kappa^2)^2} - \frac{9\kappa^2 \tanh^{-1}\sqrt{1 - \kappa^2}}{(1 - \kappa^2)^{5/2}}. \quad (11)$$

The variational estimate for chemical potential μ is:

$$\mu = \frac{1}{2w_\rho^2} + \frac{1}{4w_z^2} + \frac{w_\rho^2}{2\lambda^{2/3}} + \frac{\lambda^{4/3}w_z^2}{4} + 2 \frac{N[a - a_{\text{dd}}f(\kappa)]}{\sqrt{2\pi}w_\rho^2w_z}. \quad (12)$$

2.2. Local density approximation for polarized dipolar fermions

Based on a hydrodynamic description of the trapped degenerate dipolar gas of N single-component fermions each of mass m , we derived the following mean-field equation for this system [24, 25]

$$\begin{aligned} \mu\sqrt{n(\mathbf{r})} = & \left[-\frac{\hbar^2\nabla^2}{8m} + \frac{m\omega^2}{2}(\lambda^{-2/3}\rho^2 + \lambda^{4/3}z^2) \right. \\ & \left. + \mu_H + N \int U_{\text{dd}}(\mathbf{r} - \mathbf{r}')n(\mathbf{r}')d\mathbf{r}' \right] \sqrt{n(\mathbf{r})}, \end{aligned} \quad (13)$$

$$\mu_H = \frac{\hbar^2}{2m}[6\pi^2 N n(\mathbf{r})]^{2/3}, \quad (14)$$

and applied it [26] to study statics and dynamics of a trapped degenerate ^{161}Dy gas. In (13) μ is the chemical potential of the trapped gas, μ_H is the direct Hartree bulk chemical potential of a uniform gas with spherically symmetric Fermi surface, $n(\mathbf{r})$ is the density and the dipolar interaction U_{dd} and the trapping parameters λ and ω are the same as in the case of bosons.

The above consideration takes the Fermi surface to be spherical in the presence of the direct Hartree contribution to energy. However, in the presence of anisotropic

dipolar interaction the Fermi surface will be deformed [12, 13, 19, 27] and will take an ellipsoidal shape due to the exchange Fock interaction to energy. It has been shown that due to this deformation of the Fermi surface, the constant Fermi wave vector k_F for the noninteracting Fermi gas gets deformed to [27]

$$k(\theta) = k_F + \frac{a_{dd}}{3\pi} k_F^2 (3 \cos^2 \theta - 1). \quad (15)$$

This result is valid in the lowest order in the dipolar interaction strength a_{dd} . To this order this deformation does not change the volume of the Fermi surface or the total energy or the bulk chemical potential. This leads to the following Hartree-Fock (HF) contribution to the bulk chemical potential in the second order of interaction strength [19, 27]

$$\mu_{HF} = \mu_H - \frac{28\hbar^2}{135m} (6\pi^2)^{1/3} (3a_{dd})^2 \{Nn(\mathbf{r})\}^{4/3}. \quad (16)$$

In addition to the HF contribution to energy, there is another important contribution for the distorted Fermi surface. Kohn and Luttinger [28] showed that, in the presence of an anisotropic Fermi surface, in addition to the HF contribution the bulk chemical potential another contribution from the Brueckner-Goldstone (BG) formula could be important. Lee and Yang [29] showed that the usual BG second-order perturbative correction $E_{BG}^{(2)}$ to the ground-state energy of a dipolar Fermi gas has the following form:

$$E_{BG}^{(2)} = \sum_{m \neq 0} \frac{\langle 0 | U_{dd} | m \rangle \langle m | U_{dd} | 0 \rangle}{E_0 - E_m}, \quad (17)$$

where $|0\rangle$ and $|m\rangle$ are the ground and excited states of the noninteracting Fermi gas. This term has been evaluated by Monte Carlo integration and contributes the following to the bulk chemical potential [19]

$$\mu_{BG}^{(2)} = -\frac{14}{9} \frac{\hbar^2}{m} (3a_{dd})^2 \{Nn(\mathbf{r})\}^{4/3}, \quad (18)$$

so that the net bulk chemical potential including the HF (exchange) and BG (correlation) correction is given by

$$\mu_{HF+BG} = \mu_{HF} - \frac{14\hbar^2}{9m} (3a_{dd})^2 \{Nn(\mathbf{r})\}^{4/3}. \quad (19)$$

The quantum pressure (gradient) term in (13) contributes much less than the dominant ‘‘Fermi energy’’ term $\hbar^2[6\pi^2 Nn(\mathbf{r})]^{2/3}/(2m)$ and its neglect leads to the LDA [20, 24, 26]

$$\begin{aligned} \mu &= \frac{1}{2} m \omega^2 (\lambda^{-2/3} \rho^2 + \lambda^{4/3} z^2) + \mu_0 \\ &+ \frac{3a_{dd} N \hbar^2}{m} \int V_{dd}(\mathbf{r} - \mathbf{r}') n(\mathbf{r}') d\mathbf{r}', \end{aligned} \quad (20)$$

where we have introduced a generic bulk chemical potential μ_0 for the uniform gas which can be μ_H , μ_{HF} or μ_{HF+BG} , respectively, for spherical Fermi surface, including HF exchange correction, or including HF exchange and BG correlation correction.

A convenient dimensionless form of the LDA (20) can be obtained in terms of the scaling length $\bar{l} \equiv N^{1/6}l_0$ where $l_0 = \sqrt{\hbar/m\omega}$ is the oscillator length. Then using the scaled quantities $\bar{\rho} = \rho/\bar{l}$, $\bar{z} = z/\bar{l}$, $\bar{\mathbf{r}} = \mathbf{r}/\bar{l}$, $\bar{R} = R/\bar{l}$, $\varepsilon_{\text{dd}} \equiv 3N^{1/6}(a_{\text{dd}}/l_0) = 3N^{1/3}a_{\text{dd}}/\bar{l}$, $\bar{\mu} = \mu/(N^{1/3}\hbar\omega)$, $\bar{n}(\mathbf{r}) = n(\mathbf{r})\bar{l}^3$, (20) can be written as

$$\begin{aligned} \bar{\mu} = & \frac{1}{2}(\lambda^{-2/3}\bar{\rho}^2 + \lambda^{4/3}\bar{z}^2) + \frac{1}{2}[6\pi^2\bar{n}(\mathbf{r})]^{2/3} \\ & + \varepsilon_{\text{dd}} \int \frac{1 - 3\cos^2\theta}{\bar{R}^3} \bar{n}(\mathbf{r}') d\mathbf{r}' - \beta\varepsilon_{\text{dd}}^2[\bar{n}(\mathbf{r})]^{4/3}, \end{aligned} \quad (21)$$

with $\int d\bar{\mathbf{r}}\bar{n}(\mathbf{r}) = 1$, where $\beta = 0$ for Hartree, $\beta = 28(6\pi^2)^{1/3}/135$ for HF, and $\beta = 28(6\pi^2)^{1/3}/135 + 14/9$ for HF+BG. The scaled equation (21) is now independent of N and can be solved subject to the normalization condition to determine both the chemical potential and the density. This N -independent universal scaling (21) of the hydrodynamical equation (13) has been possible only in the LDA (20) after neglecting the quantum pressure term.

3. Numerical Result for Stability

3.1. Dipolar BEC

The dipolar BEC is known to be unstable to collapse [30] beyond a critical strength of dipolar interaction independent of trap symmetry even for repulsive contact interaction (positive values of scattering length a). In this study we consider repulsive contact interaction only. In variational equations (8) and (9) the contribution of the nonlocal dipolar interaction is reduced to a repulsive or attractive contribution contained in the terms $-a_{\text{dd}}g(\kappa)$ and $-a_{\text{dd}}h(\kappa)$ similar to the contribution of the contact interaction through the scattering length a . In these equations the aspect ratio $\kappa =, <$ and > 1 , corresponds to a spherical, cigar, and disk shape, respectively. Note that as κ changes from 0 (extreme cigar shape) to ∞ (extreme disk shape), $g(\kappa)/2$ and $h(\kappa)$ change from 1 to -2 while λ changes from 0 to ∞ . The variational approximation is an oversimplification of the actual state of affairs in case of dipolar interaction and fails to predict collapse in several cases. Improved variational ansatz [31] with time-dependent coupled Gaussian functions combined with spherical harmonics has been suggested and used in this context. In extreme cigar shape the variational contribution of the dipolar interaction is attractive and in extreme disk shape it is repulsive. In the disk shape one can argue erroneously that the system will always be stable for any number of atoms as parallel in-plane dipoles with dipole moments aligned perpendicular to the plane always repel and should make the system more stable. The net effect of short-range atomic and long-range dipolar interactions contained in the square brackets of (8) and (9) has to be attractive (negative) beyond a critical value for the system to collapse. For a moderate to extreme disk-shaped trap $\kappa > 1$ and the functions $g(\kappa)$ and $h(\kappa)$ in (8) and (9) are negative, and the contribution of a_{dd} is positive (repulsive), thus prohibiting any collapse. For a moderate to extreme cigar-shaped trap $\kappa < 1$ and the functions $g(\kappa)$ and $h(\kappa)$ are positive, and the net contribution of dipolar interaction in (8) and (9)

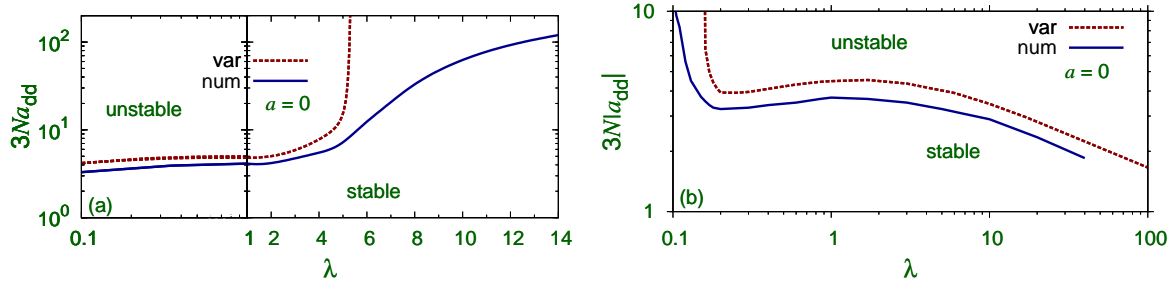


Figure 1. The critical value of the dipolar nonlinearity $3Na_{dd}$ versus the trap aspect ratio $\lambda = \omega_z/\omega_\rho$ for a stable dipolar BEC in the absence of atomic contact interaction ($a = 0$) for (a) positive and (b) negative values of the dipolar strength a_{dd} from variational approximation (var) and numerical solution (num) of the mean-field equation. Length is expressed in units of $l_0 = 1 \mu\text{m}$.

could be negative (attractive), thus leading to collapse beyond a critical value of dipolar interaction. In extreme cigar shape the functions $g(\kappa)/2$ and $h(\kappa)$ are positive but less than unity in magnitude. The quantities in square brackets in (8) and (9) are always positive (repulsive) for $a_{dd} < a$. Consequently, collapse in a cigar-shaped dipolar BEC in variational approximation is only possible for $a_{dd} > a$ and in a strongly disk-shaped BEC it is never possible. Although, the dipolar BEC is unstable to collapse for large enough N for all values of parameters, the variational approximation can only predict collapse for $a_{dd} > a$. The chemical potential and sizes predicted by the variational approximation are in good agreement with the numerical results for sets of parameters where stable BECs exist. In addition, the variational approximation may predict stable states for parameters, for which the system actually collapses.

We solve the GP equation (3) numerically by the split-step Crank-Nicolson method [32, 33]. The dipolar integral was evaluated in the Fourier momentum (\mathbf{k}) space using convolution theorem as [33]

$$\int d\mathbf{r}' V_{dd}(\mathbf{r} - \mathbf{r}') |\phi(\mathbf{r}')|^2 = \mathcal{F}^{-1} \{ \mathcal{F}[V_{dd}](\mathbf{k}) \mathcal{F}[|\phi|^2](\mathbf{k}) \}(\mathbf{r}), \quad (22)$$

where $\mathcal{F}[\]$ and $\mathcal{F}^{-1}\{ \}$ are the Fourier transform (FT) and inverse FT, respectively. The FT of the dipole potential is analytically known [33]. The FT of density $|\phi|^2$ is evaluated numerically by means of a standard fast FT (FFT) algorithm. The dipolar integral (3) is evaluated by the convolution rule (22). The inverse FT is taken by means of a standard FFT algorithm. The FFT is carried out in Cartesian coordinates and hence the GP equation is solved in three dimensions irrespective of the symmetry of the trapping potential. We use typically a space step of 0.1 and time step 0.001 and consider up to 512 points in space discretization in each direction. In our calculation we take the oscillator length $l_0 = 1 \mu\text{m}$ determined by the mass of an atom m and the angular frequency ω . The stability of the BEC in the numerical solution of the GP equation is confirmed upon obtaining a converged result after time evolution for a long time: typically an interval of time $\Delta t = 50$ (units of ω^{-1}). If a BEC survives for such a long time, usually, it stays for ever and will be termed stable.

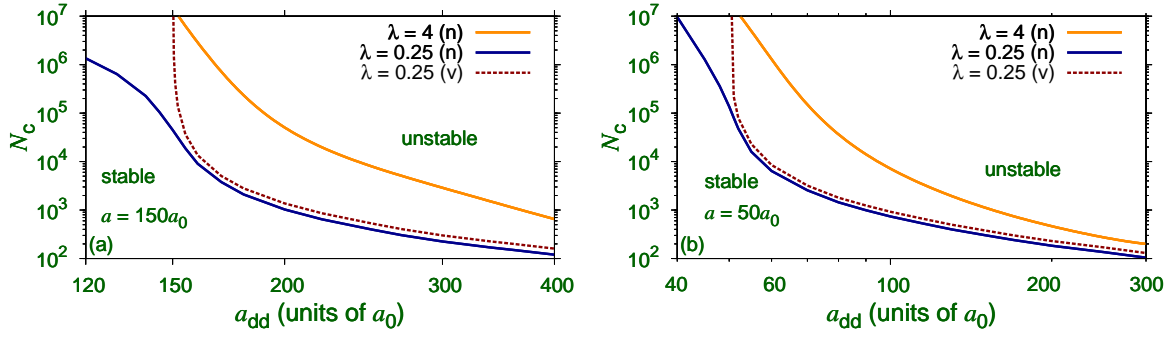


Figure 2. The critical number of atoms N_c versus the dipolar strength a_{dd} for a stable dipolar BEC with atomic S -wave scattering length (a) $a = 150a_0$ and (b) $a = 50a_0$ for trap aspect ratio $\lambda = 0.25$ and 4 from variational approximation (v) and numerical solution (n) of the mean-field equation. Oscillator unit used in calculation is $l_0 = 1 \mu\text{m}$.

First we consider the stability of the BEC after switching off the contact interaction by the Feshbach resonance technique ($a = 0$) [17]. This will show the effect of dipolar interaction alone. We consider both positive and negative values of the dipolar strength a_{dd} . The negative values of a_{dd} can be achieved by a rotating orienting field [18]. When a_{dd} is negative the dipolar interaction is attractive in disk shape and repulsive in cigar shape. So, for negative a_{dd} , the BEC is more stable in cigar shape and less in disk shape.

In figure 1 (a) and (b) we present the variational and numerical stability plots for $a = 0$ and for positive and negative values of a_{dd} , respectively, for different values of trap aspect ratio λ . The numerical results show that for all values of λ there can be collapse for both positive and negative a_{dd} . The variational results fail to predict collapse for $\lambda > 5$ in the case of positive a_{dd} and for $\lambda < 0.15$ in the case of negative a_{dd} . In these cases, variational result predicts absolute stability of the dipolar BEC, whereas the numerical result predicts a critical value of number of atoms (or of the dipolar strength a_{dd}) beyond which the dipolar BEC is unstable as shown in figures 1 (a) and (b).

We also consider stability plots in the presence of a repulsive contact interaction ($a > 0$) for positive a_{dd} . In the presence of one more variable in the system, the scattering length a , we present in figure 2 (a) the stability plot of the critical number of atoms N_c versus a_{dd} for $a = 150a_0$ for $\lambda = 0.25$ (cigar shape) and $\lambda = 4$ (disk shape), where a_0 is Bohr radius. The system collapses for $N > N_c$. The same plot for $a = 50a_0$ is shown in figure 2 (b). In both cases the variational result is also shown. The critical number of atoms N_c decreases as a_{dd} increases for both disk and cigar shapes. In both cases variational result cannot predict collapse for $\lambda = 4$ in the disk shape and predicts absolute stability for all N . For the cigar shape ($\lambda = 0.25$) the variational result predicts collapse for $a_{dd} > a$ and the variational stability line stays very close to the numerical stability line.

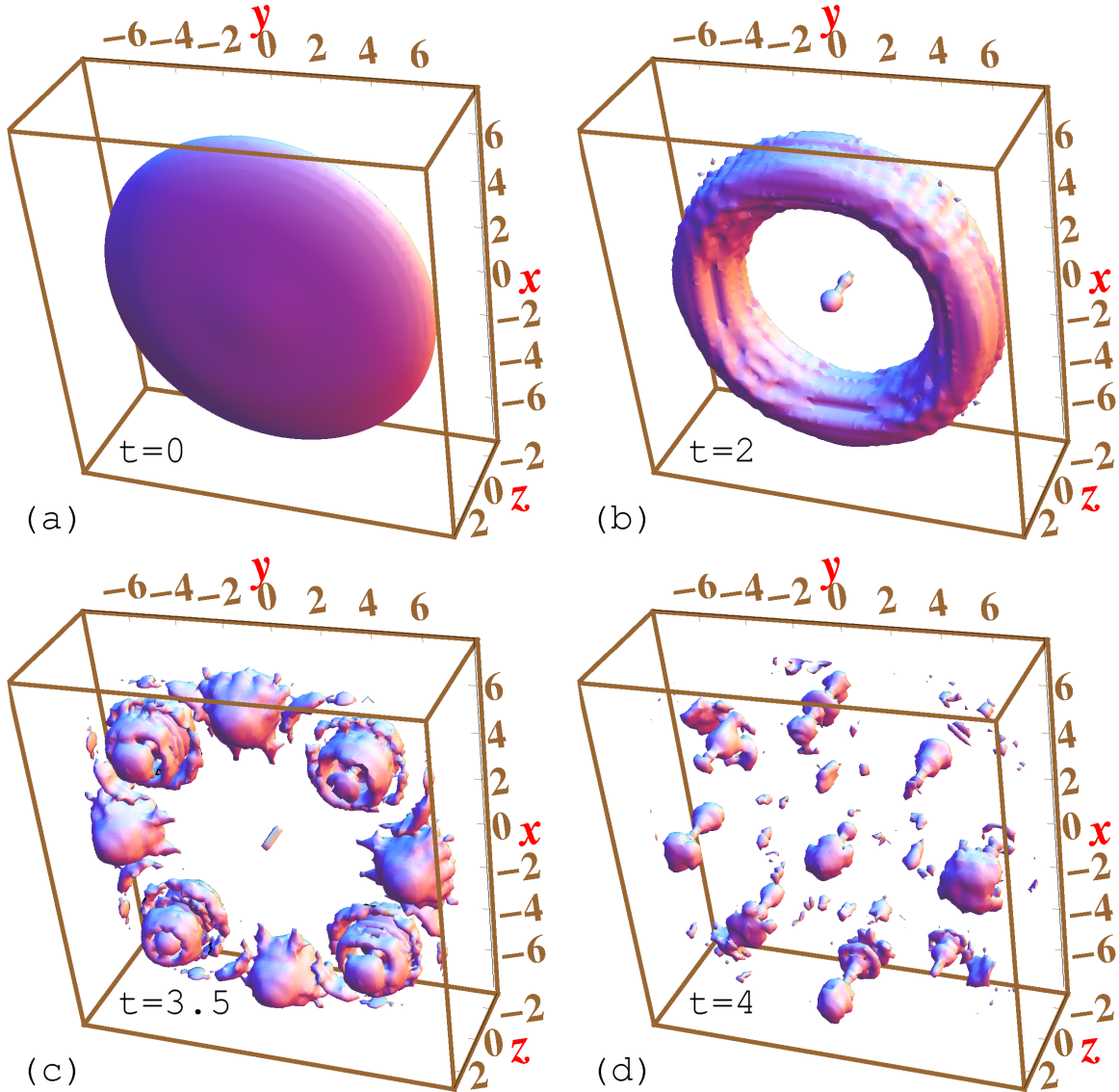


Figure 3. Dynamics to dipolar collapse: Isodensity contour of a disk-shaped dipolar BEC of 13000 ^{164}Dy atoms, with scattering length a set to zero by the Feshbach resonance technique, at times (a) $t = 0$, (b) 2, (c) 3.5, and (d) 4. The trap parameters are $\omega = 2\pi \times 60$ Hz, $\lambda = 8$, $l_0 = 1$ μm , $t_0 = 2.65$ ms. The collapse is initiated with $a_{\text{dd}} = 16a_0$. At $t = 0$ the dipolar strength a_{dd} is jumped to $a_{\text{dd}} = 40a_0$ by a rotating orienting field. The time is expressed in units of t_0 and length in units of l_0 . Density on surface of contour is 0.01 μm^{-3} .

Wilson *et al.* [8] also considered stability plot of dipolar BEC using numerical and Gaussian variational methods. Their study is, at best, complimentary to the present one. The stability plot depends on three quantities for a fixed trap aspect ratio λ : atomic scattering length a , dipolar strength a_{dd} , and number of atoms N . The study of Wilson *et al.*, more appropriate for ^{52}Cr atoms, considers instability with a variation of scattering length a for fixed N and a_{dd} . We consider instability against increase of N

for different a_{dd} . So the present study should be useful to find the maximum number of atoms in a stable dipolar BEC for different dipolar atoms and should be useful in planning future experiments. We also show the domain of applicability of the Gaussian variational method: for moderate to extreme disk shape ($\lambda > 5$) the Gaussian model always leads to stable dipolar BEC whereas the numerical analysis shows instability above a critical number of atoms.

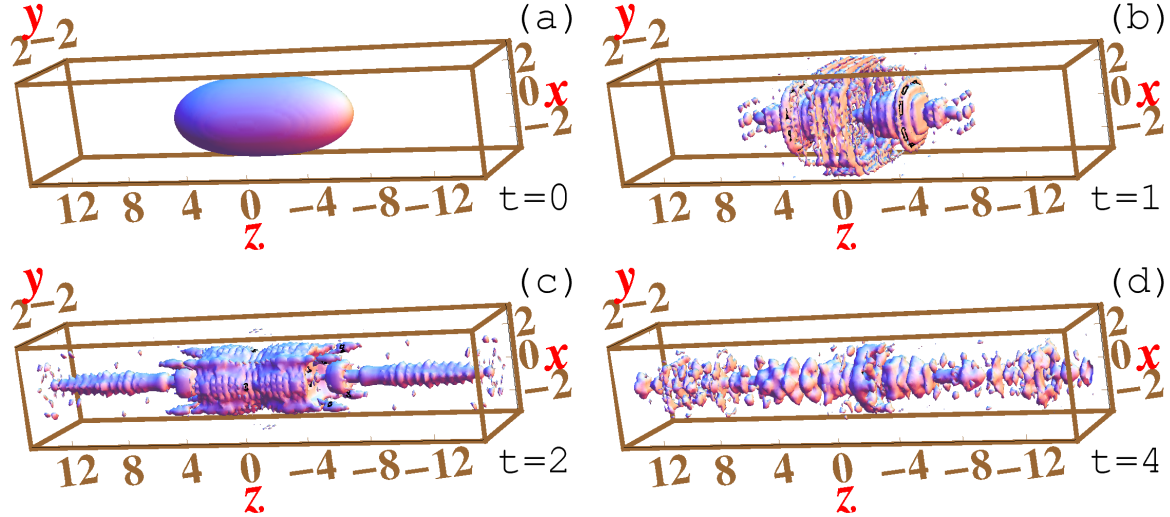


Figure 4. Dynamics to dipolar collapse: Isodensity contour of a cigar-shaped dipolar BEC of 1300 ^{164}Dy atoms, with scattering length a set to zero by the Feshbach resonance technique, at times (a) $t = 0$, (b) 1, (c) 2, and (d) 4. The trap parameters are $\omega = 2\pi \times 60$ Hz, $\lambda = 1/8$, $l_0 = 1 \mu\text{m}$, $t_0 = 2.65$ ms. The collapse is initiated with $a_{\text{dd}} = 16a_0$. At $t = 0$ the dipolar strength a_{dd} is jumped to $a_{\text{dd}} = 48a_0$ by a rotating orienting field. The time is expressed in units of t_0 and length in units of l_0 . Density on surface of contour is $0.005 \mu\text{m}^{-3}$.

Different experimental groups are trying to create a highly dipolar BEC of polar molecules [6]. The dipolar interaction strength of these molecules is typically $a_{\text{dd}} = 2000a_0$ [1]. The stability lines of figures 2 give an idea of the maximum number of these molecules in a trap with $l_0 = 1 \mu\text{m}$. A preliminary calculation indicates these numbers to be only few tens. These numbers will increase if l_0 is increased by reducing the trapping frequency ω as the critical number of molecules for stability is inversely proportional to $\sqrt{\omega}$.

Now we study the nature and dynamics of collapse in case of a disk or cigar-shaped dipolar BEC with prominent dipolar interaction by real-time evolution. In the case of spherical symmetry, the net dipolar interaction tends to average out and in that case one can have a global collapse to the center of the dipolar BEC. To study a local collapse where a dipolar BEC collapses to different local centers we consider disk- and cigar-shaped dipolar BECs with $a = 0$ and initiate the collapse by jumping a_{dd} to a larger value by a rotating orienting field [18]. In this effort, we consider ^{164}Dy atoms with $a_{\text{dd}} = 130a_0$ [3] and use the rotating orienting field to prepare an initial state

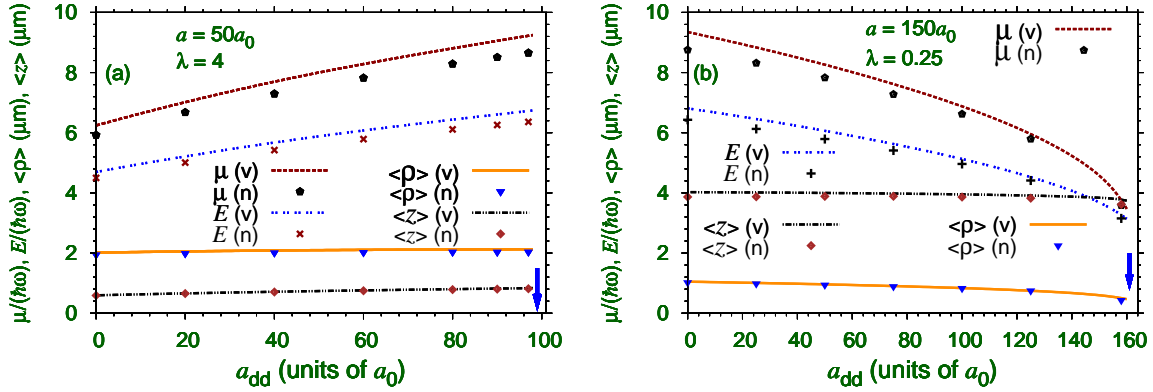


Figure 5. Chemical potential μ , energy E , and rms sizes $\langle\rho\rangle$, and $\langle z\rangle$, versus dipolar interaction strength a_{dd} of a dipolar BEC of 10000 atoms from numerical solution and variational approximation of the mean-field GP equation for (a) scattering length $a = 50a_0$ and for trap aspect ratio $\lambda = 4$ and for (b) $a = 150a_0$ and $\lambda = 0.25$. The oscillator length is taken as $l_0 = 1 \mu\text{m}$. The dark arrow on the right indicates the onset of collapse in the numerical routine at $a_{\text{dd}} = a_{\text{dd}}^{(c)}$.

with $a_{\text{dd}} = 16a_0$. The trap angular frequency ω is taken as $2\pi \times 60 \text{ Hz}$, so that the oscillator length $l_0 = 1 \mu\text{m}$. The time scale $t_0 = 2.65 \text{ ms}$. We consider $N = 13000$ atoms in a disk shaped trap with $\lambda = 8$ and initiate the collapse by jumping a_{dd} to $40a_0$ at time $t = 0$ and study the subsequent real-time evolution of the dynamics. Four snapshots of the dipolar BEC at $t/t_0 = 0, 2, 3.5$ and 4 are shown in figures 3. Due to in-plane dipolar repulsion, the atoms of the disk-shaped dipolar BEC of figure 3 (a) first moves away from center and takes a donut shape as in figure 3 (b) at $t/t_0 = 2$. Then due to strong out-of-plane attraction the donut-shaped BEC starts the process of local collapse and breaks up into small pieces as shown in figure 3 (c) at $t/t_0 = 3.5$. Finally, at $t/t_0 = 4$ these small pieces undergo collapse and break into smaller pieces which eventually occupy the whole spatial extension of the disk as shown in figure 3 (d) at $t/t_0 = 4$.

Next we study the local collapse of a cigar-shaped dipolar BEC of $N = 1300$ ^{164}Dy atoms in a trap with $\omega = 2\pi \times 60 \text{ Hz}$, $\lambda = 1/8$, $t_0 = 2.65 \text{ ms}$. The initial a_{dd} is adjusted to $16a_0$ by the rotating orienting field. A collapse is initiated by jumping a_{dd} to $48a_0$ at $t = 0$. The route to collapse is studied by real-time evolution of this dynamics as shown in figures 4. The dipolar BEC collapses on the symmetry axis, becomes elongated and eventually breaks up into small pieces at $t/t_0 = 4$ along the symmetry axis. In both cases of disk and cigar shapes we have a local collapse instead of a global collapse to the global center of the dipolar BEC.

The structures presented in figures 3 and 4 do not correspond to stationary states but to nonstationary nonequilibrium states. Although, the trapping potential has axial symmetry, we have not explicitly imposed this symmetry on the numerical solution of the GP equation. Consequently, the nonstationary nonequilibrium states of figures 3

and 4 may exhibit a small violation of this symmetry. It was noted before by Wilson *et al.* [8] that the simple Gaussian wave function assumed in (4) cannot approximate the local collapse shown, for example, in figures 3 and 4. Furthermore, Kreibich *et al.* [31] discussed this in detail and demonstrated that an improved ansatz for the stability fluctuations can overcome some of the restrictions of the Gaussian wave function. Also, the mean-field GP equation may not be fully adequate for the treatment of the multi-fragmented BEC, and a full many-body description of the dynamics might be necessary.

We also study the chemical potential and root-mean-square (rms) sizes $\langle \rho \rangle$ and $\langle z \rangle$ of disk- and cigar-shaped dipolar BECs for parameters corresponding to stability for $0 < a_{\text{dd}} < a_{\text{dd}}^{(c)}$ where $a_{\text{dd}}^{(c)}$ is the maximum value of a_{dd} beyond which the system collapses and no stationary state can be obtained. In the disk shape the variational approximation yields stable stationary state beyond this point, where the numerical routine predicts collapse. We take $a = 50a_0$ and $l_0 = 1 \mu\text{m}$ and show the present numerical and variational results for energy E , chemical potential μ , and rms sizes $\langle z \rangle$ and $\langle \mu \rangle$ of 10000 atoms in figures 5 (a) and (b) for $\lambda = 4$ (disk) and $\lambda = 0.25$ (cigar), respectively. The agreement between numerical and variational results is satisfactory in all cases. The variational energies based on energy minimization are always larger than the numerical energies.

3.2. Degenerate Fermi gas

To find the stability plot of a single-component polarized Fermi gas we use (21) valid for a large number of fermions. We solve this equation numerically without further approximation. The dipolar nonlinearity in (20) could be very large for large N , whereas the allowed values of the scaled dipolar interaction strength ε_{dd} is a small number which makes the numerical treatment of the LDA (21) a relatively easy task. This inherent symmetry of the LDA of the dipolar Fermi gas can be turned to a good advantage in the calculation of the critical number of dipolar Fermi atoms in a trapped system. The solution of the scaled equation (21) with small nonlinearity ($N = 1$) can be related to the solution of (20) for large N . We shall see that (21) permits solution for a maximum value $\varepsilon_{\text{crit}}$ of the dipolar strength ε_{dd} . This can be used to find the actual critical number of atoms N_c in a trap for a specific dipolar interaction strength a_{dd} using the scaling relation $\varepsilon_{\text{crit}} = 3N_c^{1/6}a_{\text{dd}}/l_0$.

In figure 6 (a) we plot the critical value of the scaled nonlinearity ε_{dd} versus trap aspect ratio λ for positive a_{dd} including only the direct Hartree (H) contribution, direct Hartree plus exchange Fock (HF) contribution, and finally the HF plus correlation BG (HF+BG) contribution to the energy of fermions. The direct Hartree contribution to the energy is the largest, the inclusion of the exchange and correlation corrections reduce the energy. Hence, the Hartree contribution leads to the largest critical scaled nonlinearity, the HF and HF+BG contributions lead to smaller values of critical scaled nonlinearity as can be seen in figure 6 (a). In this figure we also plot the results of Miyakawa *et al* [13] and of Zhang and Yi [12]. There is considerable discrepancy between

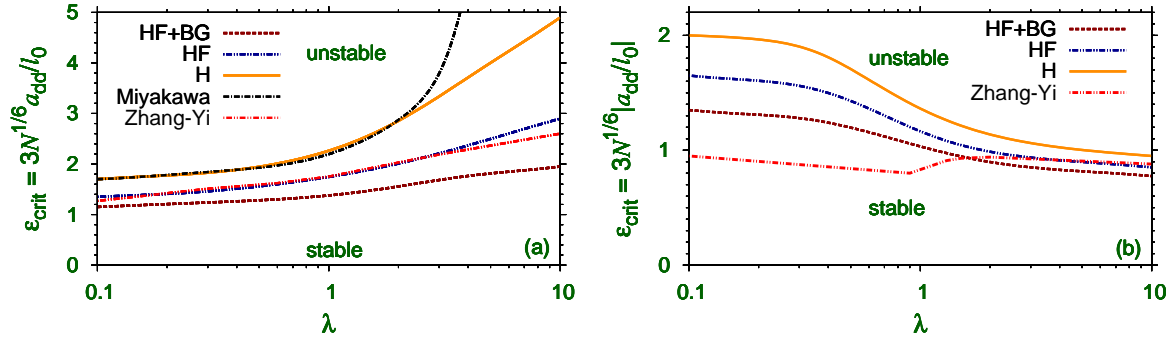


Figure 6. The critical value of the dipolar strength $\varepsilon_{\text{crit}} \equiv 3N^{1/6} a_{\text{dd}}/l_0$ versus the trap aspect ratio λ for a normal dipolar Fermi gas for both (a) positive and (b) negative a_{dd} .

these two previous calculations obtained using similar physical models, although the approximations and calculational procedure of these two studies are not identical. In view of this we consider the contribution of the different terms in the present model and compare with these previous calculations. The calculation of Zhang and Yi [12] including exchange is reasonably close to the present HF result up to $\lambda = 4$ beyond which small discrepancy is noted. The calculation of Miyakawa *et al* [13] including the HF contribution to energy is quite distinct. The latter calculation including exchange agrees with the present direct Hartree result, and not with the present HF result, up to $\lambda = 2$. The critical nonlinearity of Miyakawa *et al* including exchange for $\lambda > 2$ is much larger than the present direct Hartree result, whereas after including exchange it should be smaller. The reason for this discrepancy is not fully clear, although it could be related to the approximate variational nature of this previous calculation [34]. For positive a_{dd} the dipolar interaction is attractive in the cigar shape and repulsive in the disk shape and consequently, $\varepsilon_{\text{crit}}$ increases as λ changes from 0.1 to 10.

In figure 6 (b) we plot the same stability lines of figure 6 (a) for negative a_{dd} . In this figure we also show the stability line of Zhang and Yi [12] including exchange. Considerable discrepancy is noted between the present HF model calculation and that of Ref. [12] for $\lambda < 2$. For negative a_{dd} the dipolar interaction is attractive in the disk shape and repulsive in the cigar shape and consequently, critical ε decreases as λ changes from 0.1 to 10. However, in the stability plot of Zhang and Yi the critical values of ε for $\lambda = 0.1$ and 10 are practically the same, which does not seem physically very plausible. In view of these crucial discrepancies, further studies are needed to unveil the truth.

The stability lines of figure 6 (a) give an idea of the maximum number of polar Fermi molecules in a typical trap of oscillator length $l_0 = 1 \mu\text{m}$. Using the present HF+BG result, we can estimate the critical number of molecules for $\lambda = 0.1$ and 10 using the critical values $\varepsilon_{\text{crit}} = 1.1$ and 2.5, respectively. Using a dipolar strength $a_{\text{dd}} = 2000a_0$ [1], we obtain the critical number of molecules $N_c \approx 1700$ and 240,000, respectively, for

$\lambda = 0.1$ and 10 . As expected, these numbers are much larger than those in the case of bosonic polar molecules. The higher stability in case of the fermions is due to the Pauli exclusion principle among identical fermions.

4. Summary and Conclusion

Trapped nondipolar BECs with repulsive atomic interaction as well as trapped degenerate single-component Fermi gas are unconditionally stable. The BECs are subject to collapse instability for atomic attraction above a critical value [11]. Trapped dipolar BECs with a sufficiently strong dipolar interaction are more fragile and could be unstable to collapse independent of the underlying trap symmetry even for repulsive contact interaction [8, 9]. The condition of stability of the dipolar BECs is fully distinct. We studied the conditions of stability of dipolar BECs in axially-symmetric trap for varying trap symmetry and varying strengths of contact and dipolar atomic interactions. In all cases collapse is possible for a sufficiently large dipolar interaction. We demonstrate the local nature of dipolar collapse by real-time simulation of the collapse dynamics, where centers of local collapse develop all over the condensate and small fragments of the condensate collapse to these local centers, as opposed to a global center. We estimate the maximum number of bosonic polar molecules in a stable condensate. For a dipolar interaction strength $a_{dd} = 2000a_0$, the maximum number of molecules in a trap of oscillator length $l_0 = 1 \mu\text{m}$ is typically few tens and this number can be increased with a weaker trap.

We also studied the stability of a degenerate Fermi gas in stability plots. Independent of the underlying trap symmetry, this system will collapse for a sufficiently strong dipolar interaction [13]. The maximum number of Fermi atoms allowed in a stable system is usually much larger than that permitted in a dipolar BEC under similar conditions. We also estimate the maximum number of fermionic polar molecules in a stable system. For a typical dipolar interaction strength $a_{dd} = 2000a_0$, the maximum number of fermionic molecules in a trap of oscillator length $l_0 = 1 \mu\text{m}$ is larger than the maximum number of bosonic molecules by several orders of magnitude.

Acknowledgments

We thank FAPESP and CNPq (Brazil) for partial support.

Reference

- [1] Lahaye T *et al.* 2009 *Rep. Prog. Phys.* **72** 126401
- [2] Koch T, Lahaye T, Metz J, Frohlich B, Griesmaier A and Pfau T 2008 *Nature Phys.* **4** 218
- [3] Lu M, Burdick N Q, Youn S H and Lev B L 2011 *Phys. Rev. Lett.* **107** 190401
- [4] Aikawa K, Frisch A, Mark M, Baier S, Rietzler A, Grimm R and Ferlaino F 2012 *Phys. Rev. Lett.* **108** 210401
- [5] Lu M, Burdick N Q and Lev B L 2012 *Phys. Rev. Lett.* **108** 215301

- [6] Deiglmayr J *et al.* 2008 *Phys. Rev. Lett.* **101** 133004
de Miranda M H G *et al.* 2011 *Nature Phys.* **7** 502
- [7] Ni K K *et al.* 2008 *Science* **322** 231
Ni K K *et al.* 2010 *Nature* **464** 1324
- [8] Wilson R M, Ronen S and Bohn J L 2009 *Phys. Rev. A* **80** 023614
- [9] Ticknor C, Parker N G, Melatos A, Cornish S L, O'Dell D H J and Martin A M 2008 *Phys. Rev. A* **78** 061607
- [10] Fischer U R 2005 *Phys. Rev. A* **73** 031602
Parker N G, Ticknor C, Martin A M and O'Dell D H J 2009 *Phys. Rev. A* **79** 013617
Ronen S, Bortolotti D C E and Bohn J L 2007 *Phys. Rev. Lett.* **98** 030406
Wilson R M, Ronen S, Bohn J L and Pu H 2008 *Phys. Rev. Lett.* **100** 245302
- [11] Gammal A, Frederico T and Tomio L 2001 *Phys. Rev. A* **64** 055602
Gammal A, Tomio L and Frederico T 2002 *Phys. Rev. A* **66** 043619
- [12] Zhang J-N and Yi S 2009 *Phys. Rev. A* **80** 053614
- [13] Miyakawa T, Sogo T and Pu H 2008 *Phys. Rev. A* **77** 061603
Sogo T, He L, Miyakawa T, Yi S, Lu H and Pu H 2009 *New J. Phys.* **11** 055017
- [14] Lahaye T *et al.* 2008 *Phys. Rev. Lett.* **101** 080401
- [15] Young-S. L E and Adhikari S K 2012 *Phys. Rev. A* **86** 063611
- [16] Young-S. L E and Adhikari S K 2013 *Phys. Rev. A* **87** 013618
- [17] Inouye S, Andrews M R, Stenger J, Miesner H-J, Stamper-Kurn D M and Ketterle W 1998 *Nature* **392** 151
- [18] Giovanazzi S, Gorlitz A and Pfau T 2002 *Phys. Rev. Lett.* **89** 130401
- [19] Liu B and Yin L 2011 *Phys. Rev. A* **84** 053603
- [20] Giorgini S, Pitaevskii L P and Stringari S 2008 *Rev. Mod. Phys.* **80** 1215
- [21] Muruganandam P and Adhikari S K 2012 *Laser Phys.* **22** 813
- [22] Pérez-García V M, Michinel H, Cirac J I, Lewenstein M and Zoller P 1997 *Phys. Rev. A* **56** 1424
- [23] Huepe C *et al.* 1999 *Phys. Rev. Lett.* **82** 1616
Adhikari S K and Muruganandam P 2012 *J. Phys. B: At. Mol. Opt. Phys.* **45** 045301
- [24] Adhikari S K and Salasnich L 2008 *Phys. Rev. A* **78** 043616
Salasnich L and Toigo F 2008 *Phys. Rev. A* **78** 053626
- [25] Nygaard N and Molmer K 1999 *Phys. Rev. A* **59** 2974
Adhikari S K 2004 *Phys. Rev. A* **70** 043617
Adhikari S K 2008 *Phys. Rev. A* **77** 045602
Adhikari S K 2005 *Phys. Rev. A* **72** 053608
Capuzzi P, Minguzzi A and Tosi M P 2003 *Phys. Rev. A* **67** 053605
Capuzzi P, Minguzzi A and Tosi M P 2003 *Phys. Rev. A* **68** 033605
- [26] Adhikari S K 2012 *J. Phys. B: At. Mol. Opt. Phys.* **45** 235303
- [27] Ronen S and Bohn J L 2010 *Phys. Rev. A* **81** 033601
- [28] Kohn W and Luttinger J M 1960 *Phys. Rev.* **118** 41
- [29] Lee T D and Yang C N 1957 *Phys. Rev.* **105** 1119
- [30] Yi S and You L 2001 *Phys. Rev. A* **63** 053607
Santos L, Shlyapnikov G V and Lewenstein M 2003 *Phys. Rev. Lett.* **90** 250403
- [31] Kreibich M, Main J and Wunner G 2012 *Phys. Rev. A* **86** 013608
- [32] Muruganandam P and Adhikari S K 2009 *Comput. Phys. Commun.* **180** 1888
Vudragovic D, Vidanovic I, Balaz A, Muruganandam P and Adhikari S K 2012 *Comput. Phys. Commun.* **183** 2021
- [33] Góral K and Santos L 2002 *Phys. Rev. A* **66** 023613
- [34] Pu H 2013 *private communication*